# Dynamics of capillary flow in an undulated tube

Cite as: Phys. Fluids **33**, 052109 (2021); https://doi.org/10.1063/5.0048868
Submitted: 27 February 2021 . Accepted: 14 April 2021 . Published Online: 11 May 2021

Jiechao Lei (雷杰超 ), Zhimin Xu (徐志敏 ), Fengxian Xin (辛锋先 ), and Tian Jian Lu (卢天健 )

Physics of Fluids ARTICLE scitation.org/journal/phf

# Dynamics of capillary flow in an undulated tube

Cite as: Phys. Fluids **33**, 052109 (2021); doi: 10.1063/5.0048868
Submitted: 27 February 2021 · Accepted: 14 April 2021 ·
Published Online: 11 May 2021

View Online Export Citation CrossMark

Jiechao Lei (雷杰超),[1,2] Zhimin Xu (徐志敏),[1,3] Fengxian Xin (辛锋先),[3,4] and Tian Jian Lu (卢天健)[1,2,3,a)]

## AFFILIATIONS

[1]State Key Laboratory of Mechanics and Control of Mechanical Structures, Nanjing University of Aeronautics and Astronautics, Nanjing 210016, People's Republic of China
[2]MIIT Key Laboratory of Multifunctional Lightweight Materials and Structures, Nanjing University of Aeronautics and Astronautics, Nanjing 21006, People's Republic of China
[3]State Key Laboratory for Strength and Vibration of Mechanical Structures, Xi'an Jiaotong University, Xi'an 710049, People's Republic of China
[4]MOE Key Laboratory for Multifunctional Materials and Structures, Xi'an Jiaotong University, Xi'an 710049, People's Republic of China

[a)]Author to whom correspondence should be addressed: tjlu@nuaa.edu.cn

## ABSTRACT

From biology to engineering, while numerous applications are based on capillary phenomena in tubes having roughened surfaces, such as blood transport, paper-based rapid diagnostics, microfluidic fuel cells, and shale gas transport, the dynamics of such capillary flow remains poorly understood. We present a theoretical model for a circular undulated tube that has an idealized cosine-type inner wall characterized by two key morphological parameters: undulation amplitude and axial wave number. With the tube oriented at an arbitrary angle, we first characterize the apparent contact angle of the fluid as a function of local distortion angle and then establish a theoretical model involving inertia, viscosity, and gravity to describe the dynamics of capillary flow. A dimensionless number combining the three forces is introduced to quantify their influence. The model predictions reveal that, in an undulated tube with large wave numbers, the capillary height in equilibrium state is generally lower than that in a smooth tube of similar dimensions, whereas the reverse holds if the wave number becomes relatively small. When the viscosity of fluid is sufficiently small, capillary oscillation in an undulated tube is alleviated relative to that in a smooth tube, and hence stable capillary flow forms more easily in the former.



## I. INTRODUCTION

Numerous applications in a wide range of fields from biology, geophysics to engineering are based on the phenomena of capillary flow in small channels, such as blood transport,[1] paper-based rapid diagnostics,[2] microfluidic fuel cells,[3] functional hydrogels,[4] shale gas transport,[5] and bio-printing.[6] Often, for such applications, the channels (i.e., tubes) in which the fluids undergo capillary rise (or fall) may not be smooth but exhibit undulated (roughened) inner walls. For instance, varicose, sinuous, or sausage-like geometries are frequently found in pathologies of tracheal tubes, renal tubes, or arteries, which change the fundamental behavior of fluid flow.[7] It is therefore important to investigate, both theoretically and experimentally, the dynamics of capillary flow in undulated channels, so as to better understand the capillary phenomenon and exploit it in technologies such as heart pumps.[8]

Capillary flow in a wide variety of channels has been extensively studied under the assumption of smooth channel walls, as comprehensively reviewed by Washburn[9] and Bosanquet,[10] among others. Washburn presented an equation to quantify the capillary height in a circular smooth tube, which was subsequently validated experimentally.[9] However, the Washburn equation does not consider inertia, which leads to an unphysical infinite velocity of imbibition, making it inapplicable on long timescales. Bosanquet[10] addressed the issue by taking into account the inertia term. Recently, to better understand the problem, the Buckingham $\pi$ theorem was used to perform dimensionless analysis of dynamic capillary rise in a smooth tube.[11] Upon introducing an aspect ratio, similar dimensionless analysis was applied to characterize capillary flow in a rectangular channel.[12] Most recently, capillary rise in a smooth tube was studied, both experimentally and theoretically.[13,14] Nonetheless, as existing research predominantly focused on capillary flow in smooth tubes, how changes in the contact angle affect the dynamics of capillary flow in tubes with undulated walls needs to be quantified.[15,16]

Investigating how a liquid spreads over a rough surface, Wenzel proposed a roughness factor for contact angle measurement,[17] which

was verified experimentally.[18] Since then, the Wenzel contact angle has been widely used to describe the contact behavior of fluid on rough surfaces.[18–21] Built upon the Wenzel contact angle, several studies also directed efforts to capillary flow in undulated channels. For instance, horizontal capillary flow in conical and parabolic channels (or tubes) as well as vertical capillary flow in a parabolic channel was studied both experimentally and theoretically,[22,23] horizontal capillary flow in a tube with sinusoidal walls was investigated using dimensionless analysis,[24] and vertical capillary flow in a channel between two plates covered with cylindrical micropillar arrays was studied experimentally.[25] However, in practice, most channels are oriented at an arbitrary angle, with vertical and horizontal channels being the limiting cases. It is therefore necessary to extend existing analyses of horizontal and vertical capillary flows to cover arbitrarily oriented tubes with undulated walls, especially the dynamic rise/fall (i.e., advancing/receding) of the flow.

In the present work, we aim to quantify the effect of undulation (i.e., surface roughness) on capillary rise in a tube oriented at an arbitrary angle. For simplicity, we assume idealized cosinoidal undulation on the inner wall of a circular tube in the axial direction and account for forces originating from inertia, viscosity, and gravity to characterize the dynamics of capillary flow. To facilitate the description of different cases of capillary rise, a dimensionless number is introduced that combines all three types of the forces. It is demonstrated that the analysis is valid when the amplitude of wall undulations is relatively small in comparison with the mean radius of the tube.

## II. MODEL OF CAPILLARY RISE

Figure 1 illustrates schematically the phenomenon of capillary rise in a circular tube with an undulated (i.e., roughened) inner wall, oriented at an arbitrary angle $\phi$ relative to the horizontal surface. For symmetry, let $0 \le \phi \le \pi/2$, with $\phi = \pi/2$ ($\phi = 0$) indicating a vertical (horizontal) tube. To facilitate mathematical modeling, we assume an idealized periodic undulation, with the radius of the undulated tube described by

$$R(z) = R_0 - e\cos\left(\frac{2\pi}{b}z\right) = R_0\left[1 - \varepsilon\cos\left(\alpha\frac{z}{R_0}\right)\right], \quad (1)$$

which can be transformed into an arbitrary function with a Fourier series. Here, $R_0$ is the mean radius of the undulated tube, the dimensionless amplitude $\varepsilon$ is the ratio of $e$ to $R_0$, $\alpha = 2\pi R_0/b$ is the dimensionless wave number of the undulation, and $e$ and $b$ are the amplitude and wavelength of the undulation, respectively. The greater $\alpha$ is, the greater is the spatial density of the undulations. Given a wetting wall surface, an incompressible viscous Newtonian fluid can be driven up by capillary force, as shown in Fig. 1.

Let $h(t)$ be the height of the meniscus at time $t$. In this study, we assume that the wall is rigid and thus does not deform as the fluid rises, and we neglect the influence of entry loss and exit loss on dynamic capillary rise. Furthermore, to avoid complications such as trapped air, complete wetting is assumed.[18,26]

The total external force acting on the fluid inside a tube equals the rate of change of momentum[10]

$$F = \frac{d(m\dot{h})}{dt} = F_{cap} - F_{vis} - F_g. \quad (2)$$

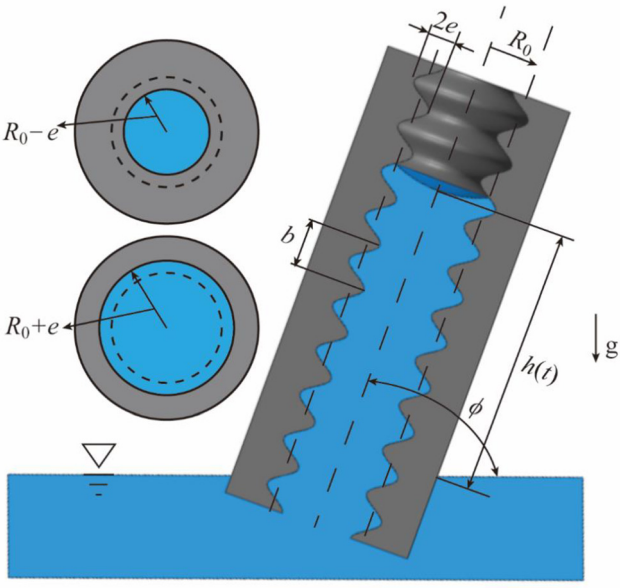


**FIG. 1.** Capillary rise in a circular tube with a cosinoidally undulated inner wall. $R_0$ is the mean radius of the tube, $e$ is the undulation amplitude, $b$ is the undulation wavelength, and $\phi$ ($0 \le \phi \le \pi/2$) is the orientation angle of the tube.

The negative signs preceding $F_{vis}$ and $F_g$ indicate that, together, the viscous force and the gravity counter the rise of the fluid, thereby doing negative work as it rises. To quantify the effect of undulation on the height to which the fluid rises, we derive the relationship between the three forces in Eq. (2) and $h(t)$.

In the first place, the rate of change in momentum is given by

$$F = \frac{d(m\dot{h})}{dt} = \frac{d\left(\pi\rho\int_0^h R^2(z)dz\dot{h}\right)}{dt} = \pi\rho R_0^2\frac{d\left(\int_0^h\left[1-\varepsilon\cos\left(\alpha\frac{z}{R_0}\right)\right]^2 dz\dot{h}\right)}{dt}, \quad (3)$$

where $m$ is the mass in a control volume enclosed by the undulated wall, $z = 0$ and $z = h$, and $\rho$ is the fluid density.

Next, to determine the apparent contact angle between the fluid surface and the undulated surface, we consider a local distortion of the contact line. As shown schematically in Fig. 2, the apparent contact angle $\varphi$ gradually changes with position on the wall from the advancing state to the receding state. For both cases (i.e., positive slope and negative slope), the apparent contact angle can be expressed as

$$\varphi = \theta + \arctan\left(\frac{dR}{dz}(h)\right) = \theta + \arctan\left[\alpha\varepsilon\sin\left(\alpha\frac{h}{R_0}\right)\right], \quad (4)$$

where $\theta$ is the static contact angle. Next, by using the Young–Laplace equation, the capillary force exerted on the fluid in the undulated tube is given by

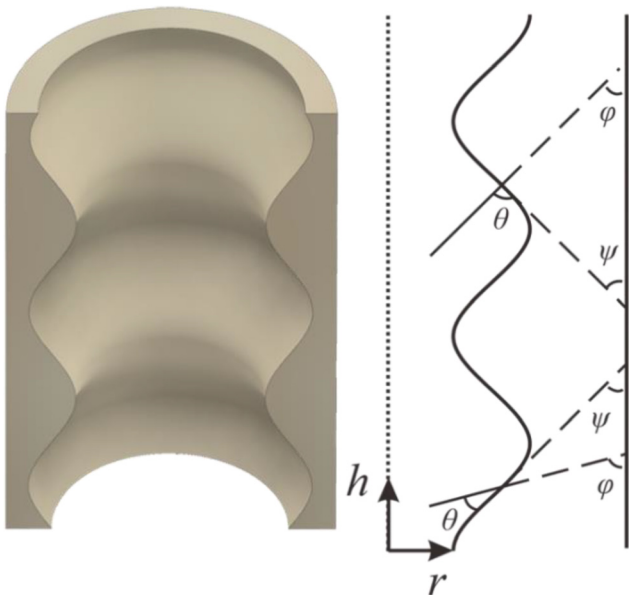


**FIG. 2.** The apparent contact angle $\varphi$ on the undulated inner surface of a circular tube gradually changes with tube position $h$. The origin of the cylindrical coordinates is placed at the tube center ($r = 0$ and $z = 0$).

$$F_{cap} = 2\gamma \frac{\cos(\varphi)}{R(h)} \pi R^2(h) = 2\pi R_0 \gamma \cos(\varphi) \left[1 - \varepsilon \cos\left(\alpha \frac{h}{R_0}\right)\right], \tag{5}$$

where $\gamma$ is the fluid surface tension.

At low Reynolds numbers, the Hagen–Poiseuille equation remains valid for $|dR/dz| = \varepsilon\alpha|\sin(\alpha z/R_0)| \ll 1$,[23] so the fluid velocity along the axis of the undulated tube is given by

$$w(r) = \frac{1}{4\eta}(r^2 - R^2)\frac{dp}{dz}, \tag{6}$$

where $\eta$ is the dynamic viscosity of the fluid, and $r$ is the radial position in cylindrical coordinates.

For $0 \le |\sin(\alpha z/R_0)| \le 1$, the product of $\varepsilon$ and $\alpha$ having a value less than 0.3 can ensure the validity of the H-P equation under all situations. However, the validity is not limited to that: for example, when $|\sin(\alpha z/R_0)| = 0.01$ and $\varepsilon\alpha = 30$, $|dR/dz| = 0.3 \ll 1$. For global validity, $\varepsilon$ and $\alpha$ should have values in reasonable ranges to ensure that the product of them is less than 0.3, as shown in Table I.

For a circular tube, the volumetric flow rate is given by

**TABLE I.** The relationship between $\varepsilon$ and $\alpha$ which ensures the global validity of the Hagen–Poiseuille equation.

| $\varepsilon$ | 0.001 | 0.01 | 0.1 | 0.3 | 0.5 |
|---|---|---|---|---|---|
| $\alpha$ | <300 | <30 | <3 | <1 | <3/5 |
| $\varepsilon\alpha$ | <0.3 | <0.3 | <0.3 | <0.3 | <0.3 |

$$Q = \pi R^2(h)\dot{h} = -\frac{\pi R^4(z)}{8\eta}\frac{dp}{dz}, \tag{7}$$

so the pressure gradient may be expressed as

$$\frac{dp}{dz} = -\frac{8\eta R^2(h)\dot{h}}{R^4(z)}. \tag{8}$$

From (6) and (8), the stress tension exerted on the undulated wall is

$$\tau = \eta \frac{dw}{dr}|_{r=R(z)} = \frac{R(z)}{2}\frac{dp}{dz} = -\frac{4\eta R^2(h)\dot{h}}{R^3(z)}, \tag{9}$$

and the viscous force exerted on the fluid is calculated by

$$\begin{aligned} F_{vis} &= -2\pi \int_0^h R(z)dz\tau \\ &= 2\pi \int_0^h \eta \frac{4R^2(h)\dot{h}}{R^3(z)} R(z)dz. \\ &= 8\pi\eta R^2(h)\dot{h}\int_0^h \frac{1}{R^2(z)}dz. \end{aligned} \tag{10}$$

The force exerted by fluid gravity on the control volume is

$$F_g = \pi\rho g \sin(\phi)\int_0^h R^2(z)dz. \tag{11}$$

Finally, substituting Eqs. (3), (5), (10), and (11) into Eq. (2) yields

$$\begin{aligned} &\rho \frac{d\left(\int_0^h \left[1 - \varepsilon\cos\left(\alpha\frac{z}{R_0}\right)\right]^2 dz\dot{h}\right)}{dt} \\ &= \frac{2\gamma\cos(\varphi)}{R_0}\left[1 - \varepsilon\cos\left(\alpha\frac{h}{R_0}\right)\right] - \frac{8\eta R^2(h)}{R_0^2}\dot{h}\int_0^h \frac{1}{R^2(z)}dz \\ &\quad - \frac{\rho g \sin(\phi)}{R_0^2}\int_0^h R^2(z)dz, \end{aligned} \tag{12}$$

which is the equation governing dynamic capillary rise in an undulated tube.

With the capillary force taken as a scaler, Eq. (12) can be rewritten in a more convenient form as

$$\frac{a}{f_0}\frac{d\left(\int_0^h \left[1 - \varepsilon\cos\left(\alpha\frac{z}{R_0}\right)\right]^2 dz\dot{h}\right)}{dt} + b\frac{f_1}{f_0}h\dot{h} + c\frac{f_2}{f_0}h\sin(\phi) = 1, \tag{13}$$

where

$$a = \frac{\rho R_0}{2\gamma\cos(\theta)}, \tag{14a}$$

$$b = \frac{4\eta}{R_0\gamma\cos(\theta)}, \tag{14b}$$

$$c = \frac{\rho g R_0}{2\gamma\cos(\theta)}, \tag{14c}$$

and

$$f_0(h) = \frac{\cos(\varphi)}{\cos(\theta)}\left[1 - \varepsilon\cos\left(\alpha\frac{h}{R_0}\right)\right], \tag{15a}$$

$$f_1(h) = \frac{R^2(h)}{h}\int_0^h \frac{1}{R^2(z)}dz, \tag{15b}$$

$$f_2(h) = \frac{1}{R_0^2 h}\int_0^h R^2(z)dz. \tag{15c}$$

The first, second, and third terms on the left side of Eq. (13) account for the inertial effect, the viscous effect, and the gravitational effect, respectively.

In the limit $\varepsilon = 0$, we have $R(z) = R(h) = R_0$, $f_0 = 1$, and $f_1 = 1$, and $f_2 = 1$. The problem then becomes that of capillary rise in a smooth tube, and Eq. (13) simplifies to

$$a\frac{d(h\dot{h})}{dt} + bh\dot{h} + ch\sin(\phi) = 1, \tag{16}$$

which is consistent with the result of Ref. 11. If the flow reaches steady state when $t \to \infty$, both the inertial and viscous forces vanish so that the steady-state capillary height is obtained by solving $h_{eq} = \rho g R_0/[2\gamma\cos(\theta)]$ for $\phi = \pi/2$.

In the next section, we use the established theoretical model to analyze the dynamic process of capillary flow in the undulated tube of Fig. 1.

## III. NUMERICAL RESULTS AND DISCUSSION

Equation (13) governs the dynamics of capillary rise in an undulated tube oriented at an arbitrary angle. However, at different stages of the fluid rise, one of the three forces due to inertia, viscosity, or gravity is relatively weak compared with the other two and thus may be neglected when solving Eq. (13). For example, the force due to gravity is relatively small during the initial stage[10] or in a microgravity environment, whereas the inertial effect can be neglected when the rising height $h > 0.1h_{eq}$.[11] Moreover, the viscous effect is small at the onset of capillary rise[27] or for a low-viscosity fluid.

Consequently, for these three different scenarios, we can adopt the three different nondimensionalization methods previously proposed for smooth tubes.[11] Generally speaking, these methods involve scaling the problem with only two of the three forces, with the initial conditions given by $h(t=0) = 0$ and $\dot{h}(t=0) = 0$. Furthermore, to quantify the influence of inertial, viscous, and gravitational forces in each of the three scenarios (i.e., small inertia, small viscosity, and small gravity), we introduce the following dimensionless number that combines all three forces:

$$\Omega = \sqrt{\frac{b^2}{ac^2}} = \sqrt{\frac{128\gamma\cos(\theta)\eta^2}{\rho^3 g^2 R_0^5}}.$$

### A. Effect of undulation on the height of capillary rise with negligible inertia

For the case of small inertia, upon choosing the viscous and gravitational forces as the scaling parameters, the dimensionless rising height $h^*$ and the corresponding dimensionless time $t^*$ take the form

$$h^* = ch = \frac{\rho g R_0}{2\gamma\cos(\theta)}h = \frac{h}{h_0}, \tag{17a}$$

$$t^* = \frac{c^2}{b}t = \frac{\rho^2 g^2 R_0^3}{16\eta\gamma\cos(\theta)}t = \frac{t}{t_0}. \tag{17b}$$

The apparent contact angle $\varphi$ can be expressed by using $h^*$ and $t^*$ as

$$\varphi = \theta + \arctan\left[\alpha\varepsilon\sin\left(\frac{2\alpha}{\mathrm{Bo}}\cos(\theta)h^*\right)\right], \tag{18}$$

where $\mathrm{Bo} = \rho g R_0^2/\gamma$ is the Bond number,[28] which reflects the importance of gravity relative to surface tension. For many fluids, such as Castor oil or UCON™ oil, the value of Bo falls within the range of 0.6–32.[29] Thus, for illustration purposes, we assume herein Bo = 30.

In terms of dimensionless variables, Eq. (13) can be rewritten as

$$\frac{1}{\Omega^2 f_0(h^*)}\frac{d\left(\int_0^{h^*} R^{*2}(z^*)dz^*\dot{h}^*\right)}{dt^*} + \frac{f_1(h^*)}{f_0(h^*)}h^*\dot{h}^* + \frac{f_2(h^*)}{f_0(h^*)}h^*\sin(\phi) = 1, \tag{19}$$

where the dimensionless parameter $\Omega$ is put into the inertia term to control the influence of inertia. As $\Omega$ increases, the influence of inertia decreases. $\Omega = 100$ is sufficiently large to simulate typical cases of negligible inertia. Here, the tube radius is normalized to $R_0$, $R^*(z^*) = R(z)/R_0$, and the distance variable is normalized to $h_0$, $z^* = z/h_0$. The coefficients $f_0$, $f_1$, and $f_2$ can thence be rewritten in dimensionless forms as

$$f_0(h^*) = \frac{\cos(\varphi)}{\cos(\theta)}R^*(h^*), \tag{20a}$$

$$f_1(h^*) = \frac{R^{*2}(h^*)}{h^*}\int_0^{h^*}\frac{1}{R^{*2}(z^*)}dz^*, \tag{20b}$$

$$f_2(h^*) = \frac{1}{h^*}\int_0^{h^*} R^{*2}(z^*)dz^*. \tag{20c}$$

Figures 3 and 4 plot the dimensionless rising height $h^*$ as a function of dimensionless time $t^*$ for selected amplitudes ($\varepsilon = 0$, 0.05, 0.1, 0.2, and 0.3) and wave numbers ($\alpha = 0$, 5, 10, 15, and 20), at $\phi = \pi/2$ (vertical tubes) and $\phi = \pi/4$ (inclined tubes), respectively. When $\varepsilon = 0$, the present result is consistent with the classical Washburn solution for smooth tubes, given by[9]

$$t^* = -h^* - \ln(1 - h^*). \tag{21}$$

The results shown in Figs. 3 and 4 show that the height of capillary rise increases with time, eventually reaching steady state where the gravity balances the capillary force. For large wave numbers (cf. $\alpha = 10$), the steady-state height decreases with increasing undulation amplitude $\varepsilon$, but increases with increasing $\varepsilon$ when $\alpha$ is relatively small (cf. $\alpha = 5$) [see Figs. 3(a) and 4(a)]. In other words, the static flow resistance increases when the undulation is denser and the amplitude is larger. Possible reasons for this observation will be discussed in detail later by studying how the steady-state height varies as a function of $\varepsilon$ and $\alpha$.

Comparing Fig. 3 with Fig. 4 shows that the steady-state height in an inclined tube *exceeds* that in a vertical tube with the same undulation structure. This occurs because, to balance the capillary force, the

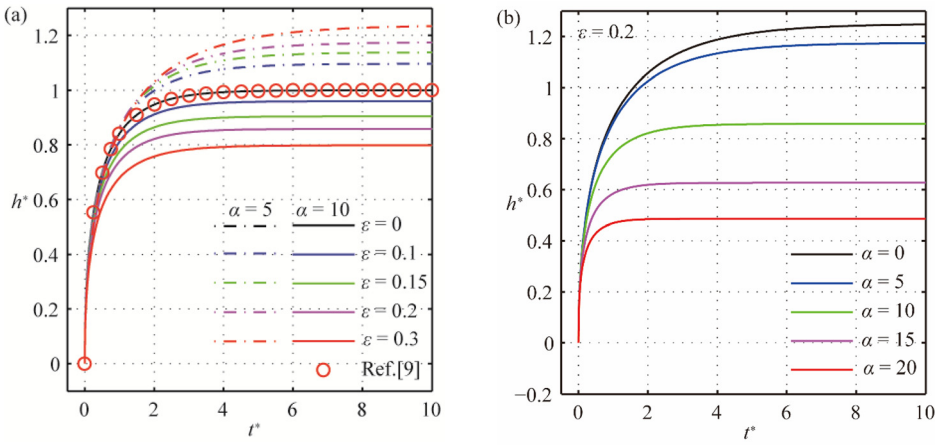


**FIG. 3.** Dynamic rising in the small-inertia case ($\Omega = 100$, $\phi = \pi/2$) for selected undulation amplitudes and wave numbers: (a) $\alpha = 5$ and 10 and (b) $\varepsilon = 0.2$ (from top, $\alpha = 0$, 5, 10, 15, and 20).

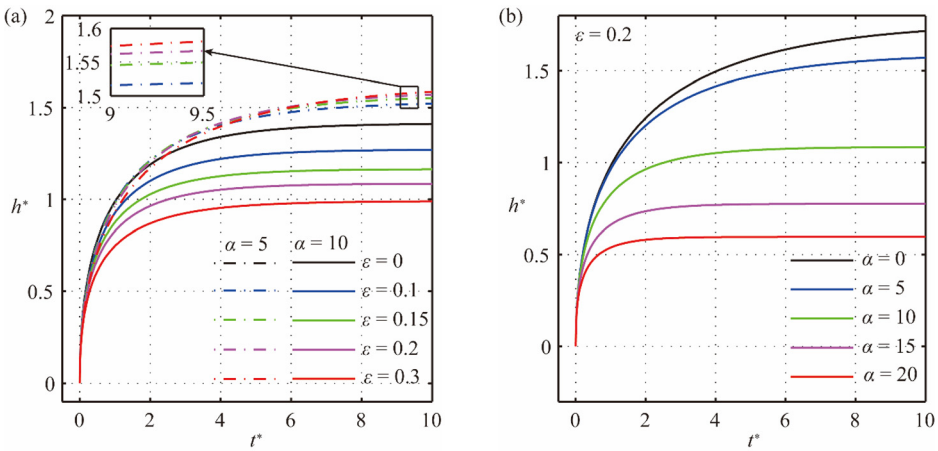


**FIG. 4.** Dynamic fluid rise in the small-inertia case ($\Omega = 100$, $\phi = \pi/4$) for selected undulation amplitudes and wave numbers: (a) $\alpha = 5$ and 10, and (b) $\varepsilon = 0.2$ (from top, $\alpha = 0$, 5, 10, 15, and 20).

fluid in the inclined tube needs to rise higher to experience the same force of gravity as in the vertical tube.

Figure 5 shows the contour lines of steady-state height with varying amplitude $\varepsilon$ and wave number $\alpha$. Note that the steady-state height in an undulated tube equals that in a smooth tube if $h^* = 1$. Figure 5 shows that the steady-state height is less than 1 for sufficiently large $\alpha$ ($\alpha > 8$) and $\varepsilon > 0.05$. Under such conditions, the wall undulation is so dense that numerous positions are available with a large radius ($R_0 + e$) for the fluid to crossover, thereby reducing the capillary force. Nevertheless, when the wave number $\alpha$ becomes sufficiently small ($\alpha < 8$), the wavelength becomes so large that the radius of the local position on the undulated surface remains almost unchanged during the whole rising process. This, together with the fact that the radius $R_0 - e$ is less than $R_0$, induces a larger capillary force, leading to a higher steady-state height ($h^* > 1$).

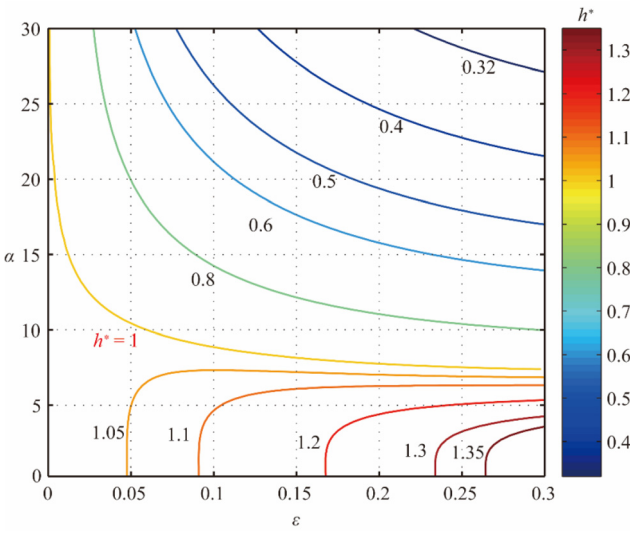


**FIG. 5.** Contours of steady-state fluid height in small-inertia case ($\Omega = 100$, $\phi = \pi/2$).

## B. Effect of undulation on the height of capillary rise with negligible viscosity

For the case of negligible viscosity, the inertial and gravitational forces are taken as the scaling parameters, so the dimensionless rising

height $h^*$ and the corresponding dimensionless time $t^*$ can be expressed as

$$h^* = ch = \frac{\rho g R_0}{2\gamma \cos(\theta)} h = \frac{h}{h_0}, \tag{22a}$$

$$t^* = \sqrt{\frac{c^2}{a}} t = \sqrt{\frac{\rho g^2 R_0}{2\gamma \cos(\theta)}} t = \frac{t}{t_0}. \tag{22b}$$

We must note that, due to the choice of different scaling parameters, $t_0$ in (22b) is different from the one in the case of negligible inertia [cf. Eq. (17b)], so the dimensionless times $t^*$ in the two cases are not identical. Since the main purpose of this study is to investigate the effect of undulation on capillary rise in different cases, we do not discuss the consecutiveness of $t^*$. Substituting (22) in Eq. (13) yields

$$\frac{1}{f_0(h^*)} \frac{d\left(\int_0^{h^*} R^{*2}(z^*) dz^* \dot{h}^*\right)}{dt^*} + \Omega \frac{f_1(h^*)}{f_0(h^*)} h^* \dot{h}^* + \frac{f_2(h^*)}{f_0(h^*)} h^* \sin(\phi) = 1, \tag{23}$$

where $\Omega$ is put into the viscous term to regulate the influence of viscosity. Decreasing $\Omega$ decreases the influence of viscosity. In the present study, we take $\Omega = 0.1$ to represent cases of negligible viscosity.

It is noticed that, at the onset of capillary rise, the viscosity force is negligible. As shown in Fig. 6(a), when $\varepsilon = 0$, the present results are entirely consistent with the analytical solution presented by Quéré for smooth tubes,[27]

$$h^* = t^* \left(1 - \frac{t^*}{6}\right). \tag{24}$$

Alternatively, when the viscosity of fluid is small, the rising height first increases, then oscillates, and finally tends to steady state with increasing time (see Figs. 6 and 7). It is found that the ratio of maximum height to steady-state height lies within the range of 1.2–1.5 for the selected amplitude $\varepsilon$ and wave number $\alpha$. Because the viscosity is negligible, viscous damping cannot stop the flow from crossing over the steady-state position. As a result, the capillary force and the gravity require a certain time to produce the balanced state, during which the oscillation amplitude gradually decreases. In addition, the oscillation frequency increases when either $\varepsilon$ or $\alpha$ increases.

For large wave numbers, a larger undulation amplitude produces a larger static flow resistance and a larger damping for fluid flow. As a result, the steady-state height decreases with increasing $\varepsilon$, and the oscillation is alleviated (see Figs. 6 and 7). However, when the wave number is relatively small, increasing the amplitude increases the surface tension since the tube radius is reduced, which in turn increases the steady-state height.

Like the case of small inertia, we use the model to determine how the combination of undulation amplitude and wave number affects the steady-state height in the case of negligible viscosity. However, once capillary flow achieves the steady state, the gravity is balanced by the capillary force, and hence the steady-state height becomes independent of inertia and viscosity. That is, changing the viscosity of the fluid affects only the oscillation. As a result, the outcome is almost the same as that shown in Fig. 5 for the case of negligible inertia; thus, for brevity, it is not presented here.

### C. Effect of undulation on the height of capillary rise with negligible gravity

Finally, consider the effect of undulation on capillary rise when the gravity is negligible. Analogous to the other two cases discussed above, upon taking the inertial and viscous forces as scaling parameters, the relevant dimensionless variables become

$$h^* = \frac{b}{\sqrt{2a}} h = \sqrt{\frac{16\eta^2}{\rho R_0^3 \gamma \cos(\theta)}} h = \frac{h}{h_0}, \tag{25a}$$

$$t^* = \frac{b}{a} t = \frac{8\eta}{\rho R_0^2} t = \frac{t}{t_0}. \tag{25b}$$

Note that, in (25), the dimensionless rising height $h^*$ and the corresponding dimensionless time $t^*$ differ from the other two cases. Therefore, the apparent contact angle also differs, as given by

$$\varphi = \theta + \arctan\left[\alpha\varepsilon \sin\left(\frac{\alpha}{4\mathrm{Oh}} \sqrt{\cos(\theta)} h^*\right)\right], \tag{26}$$

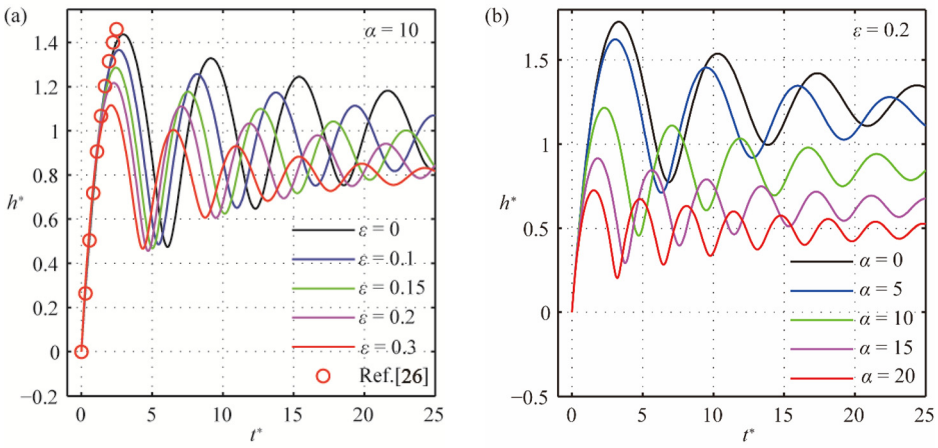


**FIG. 6.** Dynamic fluid-rise in the small-viscosity case ($\Omega = 0.1$, $\phi = \pi/2$) for selected undulation amplitudes and wave numbers: (a) $\alpha = 10$ (from top, $\varepsilon = 0$, 0.05, 0.1, 0.2, and 0.3) and (b) $\varepsilon = 0.2$ (from top, $\alpha = 0$, 5, 10, 15, and 20).

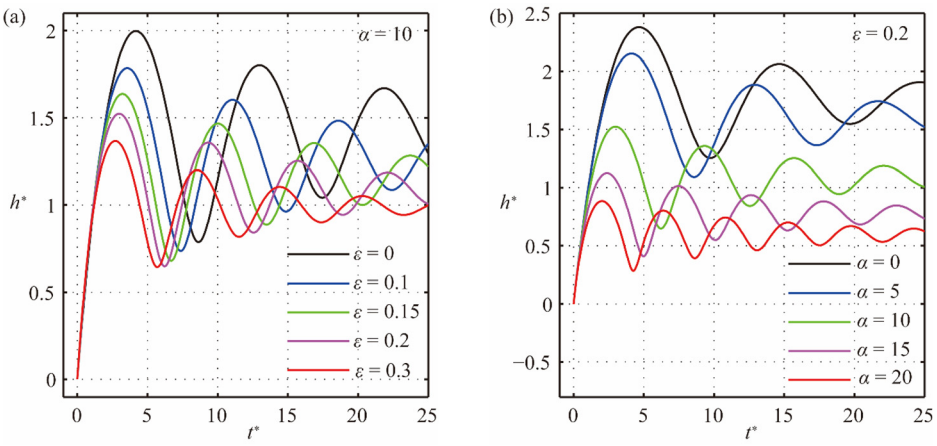


**FIG. 7.** Dynamic fluid-rise in small-viscosity case ($\Omega = 0.1$, $\phi = \pi/4$) for selected undulation amplitudes and wave numbers: (a) $\alpha = 10$ (from top, $\varepsilon = 0$, 0.05, 0.1, 0.2, and 0.3) and (b) $\varepsilon = 0.2$ (from top, $\alpha = 0$, 5, 10, 15, and 20).

where $\mathrm{Oh} = \eta/\sqrt{R_0\rho\gamma}$ is the Ohnesorge number that relates the viscous force to the inertial force and surface tension, thereby reflecting the importance of the viscous force. For instance, the viscosity, density, and surface tension of a typical lubricant oil are about $\eta = 0.13$ Pa s, $\rho = 885\,\mathrm{kg/m^3}$, and $\gamma = 25\,\mathrm{mN/m}$,[30] respectively. It follows that, when the mean radius of the tube $R_0$ lies within the range of 50–5000 $\mu$m, the Ohnesorge number can be calculated as $\mathrm{Oh} = 0.391$–$3.91$. Thus, we take $\mathrm{Oh} = 1.5$ in this study for illustration purposes.

Substituting (25) and (26) in Eq. (13) yields the dimensionless form,

$$\frac{2}{f_0(h^*)}\frac{d\left(\int_0^{h^*}\left[1-\varepsilon\cos\left(\frac{\alpha}{4\mathrm{Oh}}\sqrt{\cos(\theta)}z^*\right)\right]^2 dz^*\dot{h}^*\right)}{dt^*} + 2\frac{f_1(h^*)}{f_0(h^*)}h^*\dot{h}^* + \frac{\sqrt{2}f_2(h^*)}{\Omega f_0(h^*)}h^*\sin(\phi) = 1. \tag{27}$$

Here, the parameter $\Omega$ serves to tune the strength of the gravity effect as it appears in the third term: increasing $\Omega$ reduces the effect of gravity. We take a large enough value ($\Omega = 100$) to describe the case of negligible gravity. Thus, capillary rises in inclined and vertical tubes reach the same height at the same time.

Figure 8 plots the rising height $h^*$ as a function of $t^*$ for selected amplitudes ($\varepsilon = 0$, 0.05, 0.1, 0.2, and 0.3) and wave numbers ($\alpha = 0$, 10, 15, 20, and 30). For validation, we examine the limit $\varepsilon = 0$ and find that the present result is consistent with Bosanquet's analytical solution[10] for smooth tubes [see Fig. 8(a)],

$$h^* = \sqrt{t^* - (1 - e^{-t^*})}. \tag{28}$$

In the absence of gravity, the height does not stabilize because no force balances the capillary force, as shown in Fig. 8. In other words, the fluid continues to rise due to the absence of external forces. Similarly, the rising height decreases when either $\varepsilon$ or $\alpha$ increases, that is, when the tube is increasingly undulated.

It is interesting that, in the absence of gravity, the capillary rise in an undulated tube exhibits *stick-slip* behavior, as discussed in detail by Schäffer and Wang.[31] Moreover, if local positions with large radius $R_0 + e$ in the present undulated tube are taken as branches (as displayed schematically in Fig. 9), the stick-slip behavior occurs, as observed experimentally by Andersson *et al.*[32]

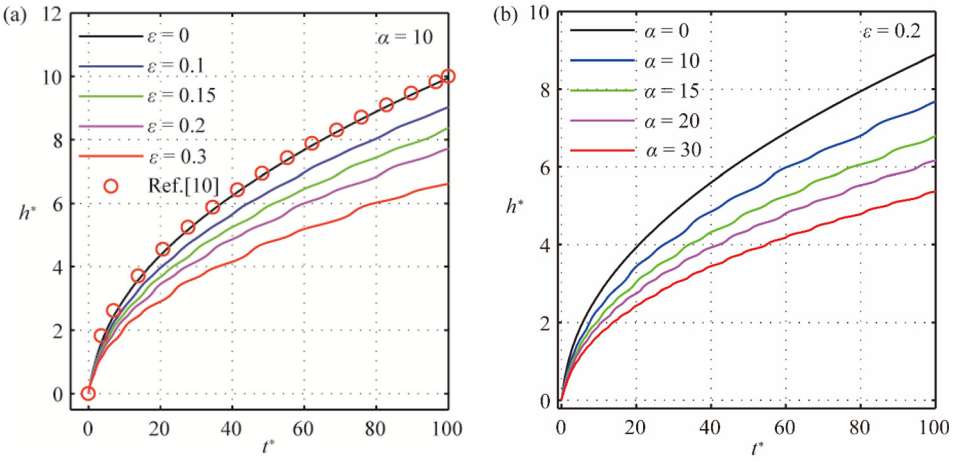


**FIG. 8.** Dynamic fluid-rise for the case of negligible gravity ($\Omega = 100$) and for selected undulation amplitudes and wave numbers: (a) $\alpha = 10$ (from top, $\varepsilon = 0$, 0.05, 0.1, 0.2, and 0.3) and (b) $\varepsilon = 0.2$ (from top, $\alpha = 0$, 5, 10, 15, and 20).

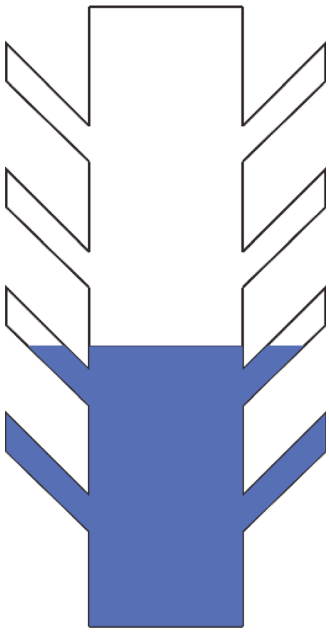

FIG. 9. Fluid rising in a tube with branches ($\phi = \pi/2$).

## IV. CONCLUDING REMARKS

We have developed an analytical model involving inertia, viscosity, and gravity to describe the dynamics of capillary rise in a circular tube with an undulated (roughened) inner wall and oriented at an arbitrary angle. With the undulation structure idealized as cosinoidal and the undulation amplitude assumed to be sufficiently small, the effect of undulation amplitude $\varepsilon$ and wave number $\alpha$ on capillary rising height has been quantified. A dimensionless number $\Omega$ combining the inertial, viscous, and gravitational forces is introduced to tune between the three different cases (i.e., small inertia, small viscosity, and small gravity) of capillary rise. Salient features drawn from the main results are summarized below:

(1) Because the apparent contact angle of the fluid varies continuously with the slope of the undulated tube wall, the capillary force differs significantly from that of a smooth tube.
(2) For negligible inertia and viscosity, the dimensionless steady-state height $h^*$ of capillary rise decreases with increasing $\varepsilon$ at large $\alpha$ ($>10$) and decreases with increasing $\alpha$ at given $\varepsilon$ (see Figs. 3, 4, 6, and 7). In contrast, the steady-state height increases ($h^* > 1$) when the undulation wave number is sufficiently small ($\alpha < 8$) (cf. Fig. 5). Moreover, the steady-state heights in these two cases are consistent with each other because they are independent of inertia and viscosity when the capillary force balances the gravity. In addition, in the case of negligible viscosity, the oscillation of capillary rise is alleviated as either $\varepsilon$ or $\alpha$ increases (see Figs. 6 and 7), and the ratio of maximum height of capillary rise to steady-state height falls within the range of 1.2–1.5 for selected values of $\varepsilon$ and $\alpha$.
(3) For the case of negligible gravity, the capillary rise does not stabilize, because no force exists to balance the capillary force (cf. Fig. 8). In this case, a stick-slip behavior occurs in the undulated tube when gravity is absent (see Fig. 8), which is consistent with previous results (Refs. 31 and 32).
(4) The steady-state height of capillary rise in an inclined tube exceeds that in a vertical tube for the cases of negligible inertia and viscosity (see Figs. 3, 4, 6, and 7).

The present results enable better understanding of the influence of undulation (surface roughness) on dynamic capillary flow, potentially significant for applications involving, e.g., blood flow in human body or fluid transport in small, roughened tubes in conventional-gravity or microgravity environments.

It needs however be pointed out that, in the present study, the influence of entry and exit losses on capillary rise has been neglected. In reality, the entry loss and exit loss both affect flow rising in a capillary tube, and there exist a number of theoretical, numerical, and experimental studies[33–38] devoted to quantifying such effects on capillary rise in a smooth tube (channel). These studies demonstrated that: (i) entrance region effects exist because the flow at the entry is not fully developed, so that the capillary pressure is less than the theoretical one; (ii) for long enough capillary tubes (tube length larger than steady capillary height), additional energy is dissipated as the capillary fluid has to displace the air, thus introducing an exit loss to decrease the capillary rate; (iii) when the tube length is less than steady capillary height, the liquid free surface exhibits oscillations at the exit of the tube. For an undulated tube, it is expected that the way that entrance pressure and exit pressure affect the dynamics of capillary rise, which is similar to its smooth counterpart. However, the effects of amplitude and density of undulation on dynamic capillary flow may be complex and need to be investigated in detail. These issues will be addressed in our future study.

## ACKNOWLEDGMENTS

This work was financially supported by the Key Program of National Natural Science Foundation of China (Grant No. 12032010), Open Fund of State Key Laboratory of Mechanics and Control of Mechanical Structure (MCMS-E-0219K02 and MCMS-I-0219K01), and by the Priority Academic Program Development of Jiangsu Higher Education Institutions (PAPD).

## DATA AVAILABILITY

The data that support the findings of this study are available from the corresponding author upon reasonable request.

## REFERENCES

[1]N. Cheewaruangroj, K. Leonavicius, S. Srinivas, and J. S. Biggins, "Peristaltic elastic instability in an inflated cylindrical channel," Phys. Rev. Lett. **122**(6), 068003 (2019).
[2]J. Songok and M. Toivakka, "Enhancing capillary-driven flow for paper-based microfluidic channels," ACS Appl. Mater. Inter. **8**(44), 30523–30530 (2016).
[3]J. P. Esquivel, F. J. Del Campo, J. L. Gómez de la Fuente, S. Rojas, and N. Sabaté, "Microfluidic fuel cells on paper: Meeting the power needs of next generation lateral flow devices," Energy Environ. Sci. **7**(5), 1744–1749 (2014).
[4]B. Grigoryan, S. J. Paulsen, D. C. Corbett, D. W. Sazer, C. L. Fortin, A. J. Zaita, P. T. Greenfield, N. J. Calafat, J. P. Gounley, A. H. Ta, F. Johansson, A. Randles, J. E. Rosenkrantz, J. D. Louis-Rosenberg, P. A. Galie, K. R. Stevens, and Jordan S. Miller, "Multivascular networks and functional intravascular topologies within biocompatible hydrogels," Science **364**(6439), 458–464 (2019).

[5]J. Y. Zuo, X. Guo, Y. Liu, Shu Pan, J. A Canas, and O. C. Mullins, "Impact of capillary pressure and nanopore confinement on phase behaviors of shale gas and oil," Energy Fuel **32**(4), 4705–4714 (2018).
[6]S. Roh, D. P. Parekh, B. Bharti, S. D. Stoyanov, and O. D. Velev, "3D printing by multiphase silicone/water capillary inks," Adv. Mater. **29**(30), 1701554 (2017).
[7]E. Hannezo, J. Prost, and J. F. Joanny, "Mechanical instabilities of biological tubes," Phys. Rev. Lett. **109**(1), 018101 (2012).
[8]M. R. Mehra, Y. Naka, N. Uriel, D. J. Goldstein, J. C. Cleveland, Jr., P. C. Colombo, M. N. Walsh, C. A. Milano, C. B. Patel, U. P. Jorde, F. D. Pagani, K. D. Aaronson, D. A. Dean, K. McCants, A. Itoh, G. A. Ewald, D. Horstmanshof, J. W. Long, and C. Salerno, "A fully magnetically levitated circulatory pump for advanced heart failure," N. Engl. J. Med. **376**(5), 440–450 (2017).
[9]E. W. Washburn, "The dynamics of capillary flow," Phys. Rev. **17**, 273–283 (1921).
[10]C. H. Bosanquet, "LV. On the flow of liquids into capillary tubes," London, Edinburgh Dublin Philos. Mag. J. Sci. **45**(267), 525–531 (1923).
[11]N. Fries and M. Dreyer, "Dimensionless scaling methods for capillary rise," J. Colloid. Interf. Sci. **338**(2), 514–518 (2009).
[12]F. F. Ouali, G. McHale, H. Javed, C. Trabi, N. J. Shirtcliffe, and M. I. Newton, "Wetting considerations in capillary rise and imbibition in closed square tubes and open rectangular cross-section channels," Microfluid. Nanofluid. **15**(3), 309–326 (2013).
[13]J. Marston, G. Toyofuku, C. Li, T. Truscott, and J. Uddin, "Drainage, rebound and oscillation of a meniscus in a tube," Phys. Fluids **30**(8), 082103 (2018).
[14]T. S. Ramakrishnan, P. Wu, H. Zhang, and D. T. Wasan, "Dynamics in closed and open capillaries," J. Fluid Mech. **872**, 5–38 (2019).
[15]M. Heshmati and M. Piri, "Experimental investigation of dynamic contact angle and capillary rise in tubes with circular and noncircular cross sections," Langmuir **30**(47), 14151–14162 (2014).
[16]P. H. Tsai, T. Kurniawan, and A. B. Wang, "A simple technique to achieve meniscus-free interfaces," Phys. Fluids **31**, 011702 (2019).
[17]R. N. Wenzel, "Resistance of solid surfaces to wetting by water," Ind. Eng. Chem. **28**(8), 988–994 (1936).
[18]J. Bico, U. Thiele, and D. Quéré, "Wetting of textured surfaces," Colloid. Surf. A **206**(1), 41–46 (2002).
[19]A. Malijevský, "Does surface roughness amplify wetting?" J. Chem. Phys. **141** (18), 184703 (2014).
[20]K. M. Hay, M. I. Dragila, and J. Liburdy, "Theoretical model for the wetting of a rough surface," J. Colloid. Interf. Sci. **325**(2), 472–477 (2008).
[21]T. Patel, D. Patel, N. Thakkar, and A. Lakdawala, "A numerical study on bubble dynamics in sinusoidal channels," Phys. Fluids **31**, 052103 (2019).
[22]M. Reyssat, L. Courbin, E. Reyssat, and H. A. Stone, "Imbibition in geometries with axial variations," J. Fluid Mech. **615**, 335–344 (2008).
[23]B. Figliuzzi and C. R. Buie, "Rise in optimized capillary channels," J. Fluid Mech. **731**, 142–161 (2013).
[24]Q. Wang, E. R. Graber, and R. Wallach, "Synergistic effects of geometry, inertia, and dynamic contact angle on wetting and dewetting of capillaries of varying cross sections," J. Colloid. Interf. Sci. **396**, 270–277 (2013).
[25]J. Kim, M. W. Moon, and H. Y. Kim, "Capillary rise in superhydrophilic rough channels," Phys. Fluids **32**(3), 032105 (2020).
[26]D. Quéré, "Wetting and roughness," Annu. Rev. Mater. Res. **38**(1), 71–99 (2008).
[27]D. Quéré, "Inertial capillarity," Europhys. Lett. **39**(5), 533–538 (1997).
[28]M. Guémas, A. Sellier, and F. Pigeonneau, "Low-Reynolds-number rising of a bubble near a free surface at vanishing Bond number," Phys. Fluids **28**, 063102 (2016).
[29]H. Kočárková, F. Rouyer, and F. Pigeonneau, "Film drainage of viscous liquid on top of bare bubble: Influence of the Bond number," Phys. Fluids **25**(2), 022105 (2013).
[30]C. T. Pinheiro, R. F. Pais, A. G. M. Ferreira, M. J. Quina, and L. M. Gando-Ferreira, "Measurement and correlation of thermophysical properties of waste lubricant oil," J. Chem. Thermodyn. **116**, 137–146 (2018).
[31]E. Schäffer and P. Wong, "Dynamics of contact line pinning in capillary rise and fall," Phys. Rev. Lett. **80**(14), 3069–3072 (1998).
[32]J. Andersson, A. Larsson, and A. Ström, "Stick–slip motion and controlled filling speed by the geometric design of soft micro-channels," J. Colloid. Interf. Sci. **524**, 139–147 (2018).
[33]C. D. Han and M. Charles, "Entrance- and Exit-Correction in Capillary Flow of Molten Polymers," Trans. Soc. Rheol. **15**, 371 (1971).
[34]G. Lu, X. D. Wang, and Y. Y. Duan, "Study on initial stage of capillary rise dynamics," Colloid Surf. A **433**, 95–103 (2013).
[35]J. F. Xiao, Y. M. Luo, M. Y. Niu, Q. Wang, J. L. Wu, X. Liu, and J. F. Xu, "Study of imbibition in various geometries using phase field method," Capillarity **2**(4), 57–65 (2019).
[36]M. Hultmark, J. M. Aristoff, and H. A. Stone, "The influence of the gas phase on liquid imbibition in capillary tubes," J. Fluid Mech. **678**, 600–606 (2011).
[37]Y. K. Kim, J. Hong, K. H. Kang, S. J. Lee, and J. Kim, "Capillary waves in a sharp-edged slit driven by vertical vibration," Exp. Therm. Fluid Sci. **71**, 52–56 (2016).
[38]H. J. Kim, M. A. Fontelos, and H. J. Hwang, "Capillary oscillations at the exit of a nozzle," IMA J. Appl. Math. **80**, 931–962 (2015).